Applied Physics Letters

Encapsulation of locally welded silver nanowire with water-free ALD-SbO_x for flexible thin-film transistors

Cite as: Appl. Phys. Lett. **121**, 163504 (2022); https://doi.org/10.1063/5.0118500
Submitted: 05 August 2022 • Accepted: 25 September 2022 • Published Online: 18 October 2022

Jun Yang, Amin Bahrami, Xingwei Ding, et al.

AIP Publishing

Applied Physics Letters ARTICLE scitation.org/journal/apl

Encapsulation of locally welded silver nanowire with water-free ALD-SbO_x for flexible thin-film transistors

Cite as: Appl. Phys. Lett. **121**, 163504 (2022); doi: 10.1063/5.0118500
Submitted: 5 August 2022 · Accepted: 25 September 2022 ·
Published Online: 18 October 2022

Jun Yang,[1,2] Amin Bahrami,[1,a)] Xingwei Ding,[3] Sebastian Lehmann,[1] and Kornelius Nielsch[1,2,a)]

AFFILIATIONS

[1]Institute for Metallic Materials, Leibniz Institute of Solid State and Materials Science, 01069 Dresden, Germany
[2]Institute of Materials Science, Technische Universität Dresden, 01062 Dresden, Germany
[3]Key Laboratory of Advanced Display and System Application, Ministry of Education, Shanghai University, 200072 Shanghai, China

Note: This paper is part of the APL Special Collection on Metal Oxide Thin-Film Electronics.
[a)]**Authors to whom correspondence should be addressed:** a.bahrami@ifw-dresden.de and k.nielsch@ifw-dresden.de

ABSTRACT

Transparent conductive electrodes are essential in the application of flexible electronics. In this work, we successfully demonstrated a novel strategy for improving mechanical/electrical properties of indium tin oxide (ITO)-free flexible silver nanowire (Ag NW) thin films. To reduce the contact resistance of Ag NWs, an ethanol-mist was used to weld the cross junction of wires at room temperature. The nano-welded Ag NWs (W-Ag NWs) were then coated with an aluminum-doped ZnO (AZO) solution, which significantly reduce the roughness of the Ag NW thin film. Finally, an ultrathin SbO_x thin film of 2 nm was deposited on the film surface using a water-free low-temperature atomic layer deposition technique to protect the W-Ag NW/AZO layer from water or oxygen degradation. The treated Ag NWs have a high transmittance of 87% and a low sheet resistance of about 15 Ω/sq, which is comparable with the ITO electrode's property. After 1000 cycles of bending testing, the W-Ag NW/AZO/SbO_x film practically retains its initial conductivity. Furthermore, the samples were immersed in a solution with pH values ranging from 3 to 13 for 5 min. When compared to untreated Ag NWs or those coated with AlO_x thin films, W-Ag NW/AZO/SbO_x had superior electrical stability. The W-Ag NW/AZO/SbO_xlayer was integrated as a gate electrode on low-power operating flexible Ti-ZnO thin film transistors (TFTs). The 5% Ti-ZnO TFT has a field-effect mobility of 19.7 $cm^2\ V\ s^{-1}$, an I_{on}/I_{off} ratio of 10^7, and a subthreshold swing of 147 mV $decade^{-1}$.

Transparent conductive electrodes (TCEs) have obtained much interest in the last few years in optoelectronic device fields, including touch screens, organic light-emitting diodes (OLEDs), and solar cells.[1–4] So far, TCEs, such as indium tin oxide (ITO),[5] aluminum-doped zinc oxide (AZO),[6] and tungsten-doped indium oxide (WIO),[7] have all been studied extensively. Among them, ITO is widely investigated because of its excellent transparency (>90%) and conductivity (<20 Ω/sq).[8] However, various drawbacks, such as brittleness, high-temperature processing, and strain sensitivity, limit its application in flexible optoelectronics. Three key issues concerning electrodes must be resolved to develop high-performance flexible optoelectronic devices: (i) low-temperature preparation, (ii) high flexibility in integrated circuits, and (iii) long-term air environment stability. Many researchers are now developing flexible transparent electrode materials. Carbon nanotubes (CNTs),[9] silver nanowires (Ag NWs),[10,11] graphene,[12] and conducting polymers[13] have all been used to make conductive films with optical transparency and mechanical flexibility to replace conventional ITO electrodes. The one-dimensional Ag NW-based electrode, which can be fabricated using a low-temperature solution preparation procedure, is the most promising contender among these alternatives with low sheet resistance, good transparency, and low manufacturing cost. Nonetheless, several obstacles must be solved before Ag NW TCEs can be used in real-world applications. To begin with, the as-prepared Ag NWs exhibit a high contact resistance at junctions due to the nanogap and weak contact, which can suppress the charge carrier transfer and introduce Joule heating at junctions.[14] Second, the surface roughness of the Ag NW layer is quite high, making current leakage in fabricated optoelectronic devices difficult to

control. Third, when exposed to a corrosive environment, the Ag NWs are easily oxidized, resulting in a significant increase in the sheet resistance.[8] Some encapsulation thin films have been studied to coat Ag NW networks to avoid water or oxygen damage such as atomic layer deposition (ALD) processed AZO or Al_2O_3.[15,16] However, during the ALD process, water or ozone is introduced, which can re-oxidize the surface of Ag NWs and increase the resistance.

Herein, several procedures were investigated in this study to address the aforementioned difficulties. To begin, a room temperature approach was developed to weld the Ag NW networks using ethanol-mist to generate nano-welded Ag NW networks (W-Ag NWs) on a hydrophilic flexible polyimide (PI) substrate. The AZO solution was then applied to reduce the roughness and improve adhesion between the Ag NW layer and the substrate. Finally, an ultrathin SbO_x thin film was deposited on the AZO/W-Ag NW layer by low-temperature ALD using a water-free recipe to passivate charge recombination defects and avoid exposure to water or oxygen. SbO_x possesses excellent dielectric properties and has a great potential for encapsulation of microelectronic devices.[17,18] Due to the self-limiting characteristics, the ALD-processed film can create a highly conformal and dense oxide coating without pinholes.[19] Thus, the ALD-SbO_x layer is perfect for protecting the Ag NWs against oxidation and corrosion. The key feature of this study is that no water is used in any phase of the device fabrication to avoid unwanted Ag NW surface oxidation. The Ag NW electrodes retain their high transmittance of 87% and a low sheet resistance of ~15 Ω/sq in harsh environments. In the final part of this research, the flexible thin-film transistors (TFTs) based on Ti-doped ZnO (Ti-ZnO) were fabricated employing W-Ag NW/AZO/SbO_x as the gate electrode. The 5% Ti-ZnO TFT possesses a field-effect mobility of 19.7 $cm^2\ V\ s^{-1}$, an I_{on}/I_{off} ratio of 10^7, and a subthreshold swing (*SS*) of 147 mV $decade^{-1}$. The inverters based on Ti-ZnO TFTs were investigated further. These exceptional device characteristics show its immense potential to be used in flexible and wearable electronics.

The existence of nanogaps and poor contact in the junctions of untreated Ag NW films, as illustrated in Figs. 1(a), 1(b), and 1(f), has a detrimental effect on the electrical characteristics and mechanical flexibility of the Ag NW films. Therefore, a welding treatment is required to minimize Joule heating and enhance mechanical properties.[20] This is accomplished in two easy steps: (i) the application of ethanol-mist and (ii) the drying procedure. The Ag NW films were simply hung face down on a beaker for a specified period at room temperature. The detailed fabrication processes can be found in the supplementary material. Under ambient conditions, the ethanol-mist reaches the junctions. When the Ag NW films dry for 30 s, the nanogap between two wires tends to form a meniscus-shaped capillary bridge, as shown in Figs. 1(a), 1(g), and S1.[21] Figure S2 depicts the nano-welding model, which is explained by the following equations:[22]

$$F = -\frac{2\pi R\gamma \cos\theta}{1 + [H/2d]}, \tag{1}$$

$$d = \frac{H}{2} \times \left[-1 + \sqrt{1 + \frac{2V}{\pi R H^2}}\right], \tag{2}$$

where F is the capillary force between two nanowires connected by a liquid bridge; R is the radius of the sphere, which is approximately equal to the radius of the Ag NW; γ is the surface tension of ethanol-mist; θ is the contact angle; H is the capillary bridge distance between two nanowires; V is the liquid volume; d is the immersion length. Given ethanol's surface tension of 21.8 mN/m, a capillary bridge with a distance of $H = 50$ nm and a typical water volume of $V = 10^3$ nm^3 with $\theta = 60°$, the F can be estimated to be ~5 nN. H becomes as small

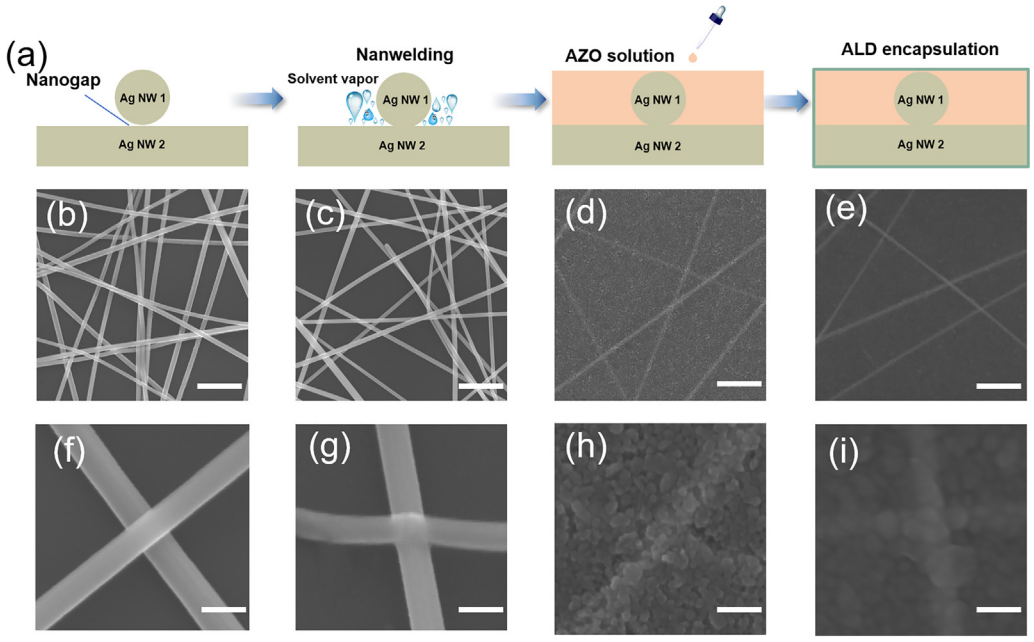

FIG. 1. (a) Schematic and SEM images of W-Ag NW thin films preparation. (b) and (f) As coated Ag NW. (c) and (g) After ethanol treatment. (d) and (h) After AZO solution coating. (e) and (i) After SbO_x coating. Scale bars for (b)–(e) are 1 μm and for (f)–(i) are 100 nm.

as several nanometers when the spacing between two nanowires constricts. In practice, the compressive pressure between two nanowires is in MPa at first and rises to GPa as the two spheres get closer. Due to the self-limited nature of the capillary-driven welding process, it happens only at the cross areas of two nanowires and does not affect others regions.[21] Therefore, the contacted nanowires could be effectively welded [Figs. 1(a), 1(c), 1(g), and S1]. The post-AZO-spin coating process resulted in the formation of the W-Ag NW/AZO core–shell structure [Figs. 1(d) and 1(h)]. Finally, a 2 nm ALD-SbO_x film was grown on the W-Ag NW/AZO layer to passivate the charge recombination defects and improve the corrosion resistance [Figs. 1(e) and 1(i)]. The surface roughness of Ag NW-based layers decreased significantly from 20.6 (Ag NW) to 3.3 nm (W-Ag NW/AZO/SbO_x), which is highly advantageous to the formation of high-quality electrode layers (Fig. S3).

For transparent electrodes, the sheet resistance and transmittance are essential parameters. In general, ITO performs effectively with a sheet resistance of ∼15 Ω/sq and a transmittance of about 90% [Figs. 2(a) and S4]. The sheet resistance and transmittance of Ag NW-containing samples were measured as a function of the nanowire concentration. The film containing 0.5 mg/ml Ag NW exhibits more than 90% transmittance with a very high resistance of ∼327 Ω/sq, rendering it unsuitable for use in optoelectronic devices. The 1.5 mg/ml Ag NW-containing sample, on the other hand, has a very low resistance of less than 10 Ω/sq but a relatively low transmittance of 80% at 550 nm. However, the 1 mg/ml Ag NW coating shows a low sheet resistance of ∼20 Ω/sq and a high transmittance of 87%, making it suitable for optoelectronic device fabrication and also a sample for further optimization in this work. Figure 2(b) shows that as the number of ethanol-mist treatments increases on the film increases, the sheet resistance of 1 mg/ml Ag NW decreases. The ethanol-mist treatment is a quick and easy way to weld the junctions and lower the resistance of Ag NWs at room temperature. As can be seen, after ten repetitions of ethanol-mist treatment, the sheet resistance was reduced significantly to half that of the unwelded coating (from ∼35 to ∼15 Ω/sq). Beyond that treatment number, the sheet resistance was not decreased further.

Another interesting observation is that the hydrophilia of the substrate show a great effect on the nano-welding process. As illustrated in Fig. 2(c), the resistance of Ag NWs coated on the hydrophobic substrate was nearly unchanged after ethanol-mist treatment. On the contrary, the resistance decreased significantly on the hydrophilic substrate, revealing that the hydrophilic substrate presented a strong adhesive force for Ag NW films. The capillary force on the hydrophobic substrate is significantly smaller than on the hydrophilic substrate.[23] Figures 2(d) and S5 demonstrate the electrical and optical characteristics of Ag NWs after each consecutive treatment. The results indicate that coating Ag NWs with an AZO solution and then a 2 nm SbO_x thin film had a negligible effect on the resistance and

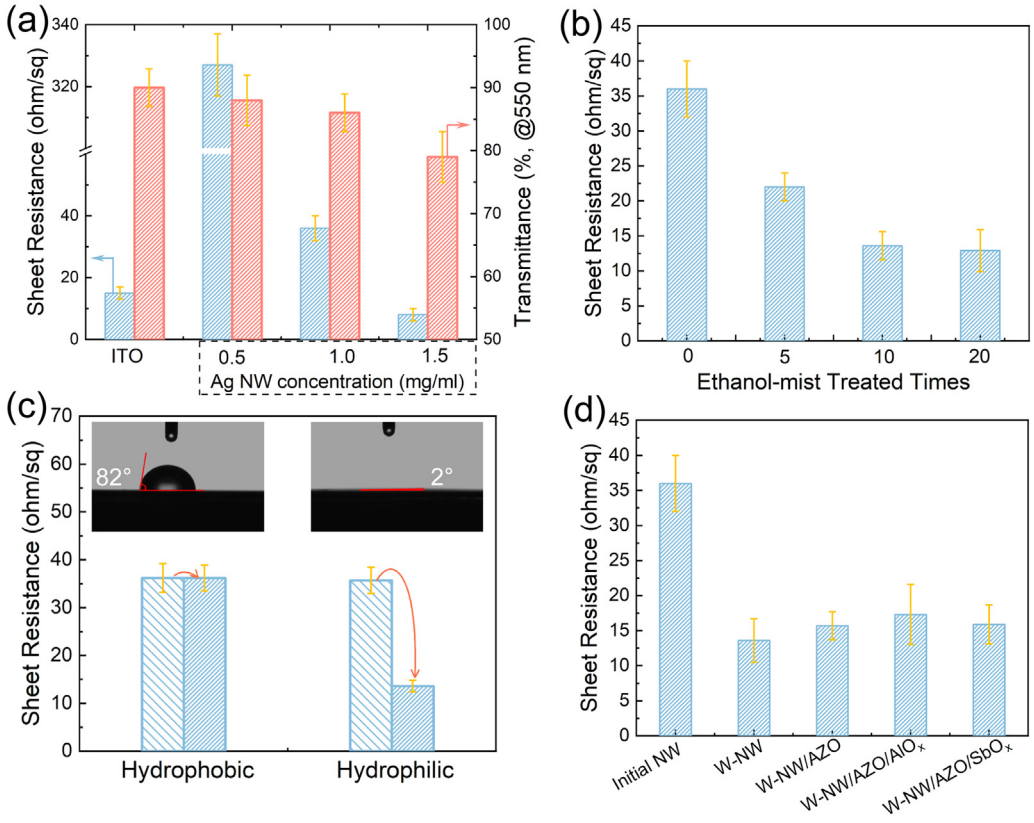

FIG. 2. (a) Sheet resistance and transmittance of Ag NWs with different concentrations. (b) Effect of ethanol-mist treatment times on the sheet resistance. (c) Sheet resistance variation of Ag NWs (1 mg/ml) with hydrophobic and hydrophilic substrates. (d) Sheet resistance and transmittance of Ag NWs with different treatment processes.

transmittance of the film. Therefore, for further characterization and optimization, the W-Ag NW/AZO/SbO_x thin film with high conductivity and optical transmittance is being explored.

Ag NW layer's sheet resistance was measured while maintaining the film at various temperatures over varying lengths of time to study the thermal stability of different structures. Figure 3(a) shows that the sheet resistance of the bare Ag NW film increased significantly after 40 min of keeping it at 250 °C. However, after being held at 250 °C for 60 min, the sheet resistance of welded and coated Ag NW films, i.e., W-Ag NW/AZO/AlO_x and W-Ag NW/AZO/SbO_x films, remained unaffected [Fig. 3(a)]. After 10 min at a higher temperature of 300 °C, the bare Ag NW turns into an insulator. Nevertheless, after 60 min of holding at 300 °C, the sheet resistance of the W-Ag NW/AZO/SbO_x thin film marginally increased from 16 to 25 Ω/sq [Fig. 3(b)]. Further increasing the temperature to 350 °C causes the sheet resistance of bare Ag NW to exceed measuring capacity, implying Ag oxidation [Fig. 3(c)].

The corrosion resistance of Ag NWs for electrode applications was also evaluated, as shown in Fig. 3(d). The bare Ag NWs and treated Ag NWs were immersed in de-ionized (DI) water with varying pH values for 5 min. The sheet resistance values in Fig. 3(d) reported are normalized to better illustrate the effect of degradation. The sheet resistance of both Ag NWs and treated Ag NWs samples did not change significantly in DI water with pH = 7. However, bare Ag NWs showed very high resistance in acidic conditions, indicating that Ag NWs were severely etched. Interestingly, in an acidic solution (pH = 13), Ag NWs encapsulated with the AlO_x layer performed worse than Ag NWs encapsulated with the water-free processed SbO_xlayer, implying that SbO_x has superior anti-corrosion characteristics in alkaline solutions than AlO_x.

Another important criterion for flexible transparent electrode materials is mechanical robustness. Figure 3(e) depicts the results of the ITO and Ag NW layer bending test. The sheet resistance of ITO increased dramatically after 1000 cycles of bending due to its brittle nature, whereas the W-Ag NW/AZO/SbO_x film maintained its conductivity even after 1000 cycles of bending, indicating the negligible impact of mechanical bending on the performance of flexible devices. This extraordinary result could be explained by three considerations: (i) The brittle nature of ITO makes it vulnerable against bending loads; (ii) bending of layers generates abundant fractures in the nano-welded

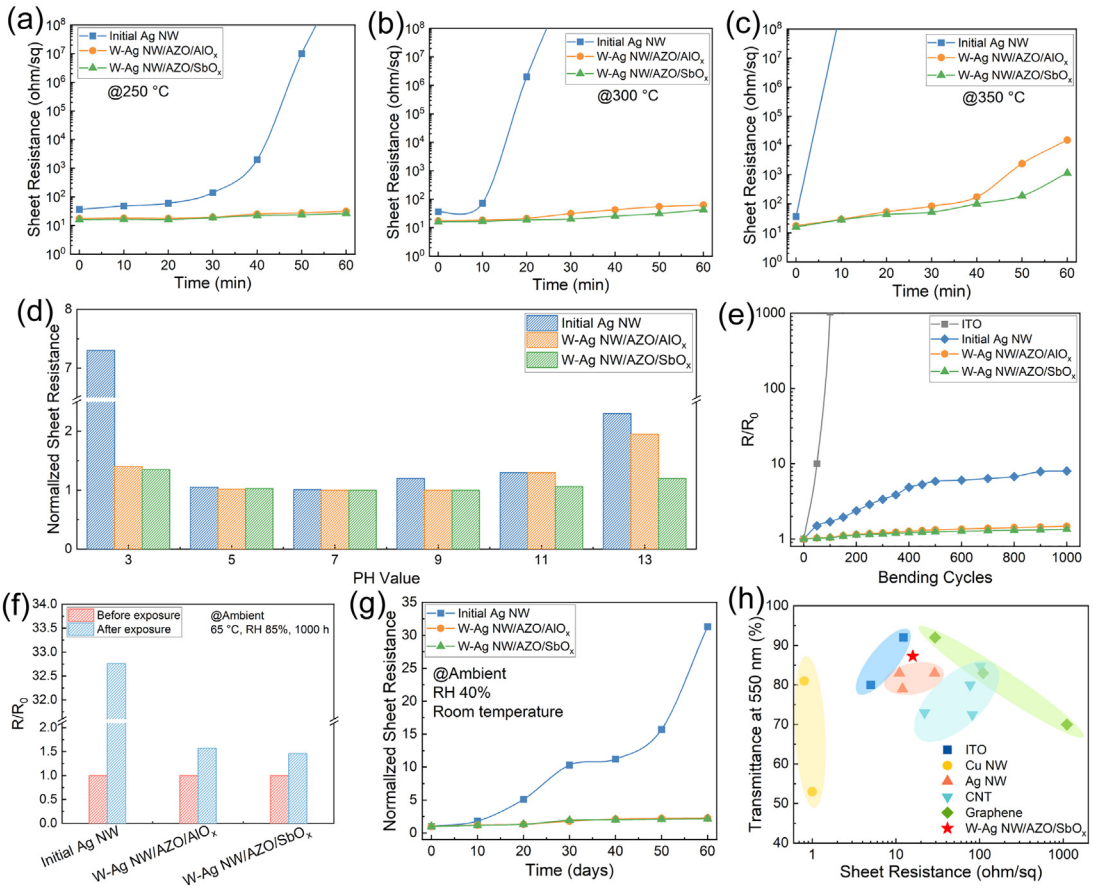

FIG. 3. (a)–(c) Thermal and (d) chemical corrosion stabilities of Ag NWs. (e) Mechanical stability of Ag NWs coated on the PI substrate. (f) Ambient and (g) long-term tested stabilities of Ag NWs. (h) Sheet resistance vs optical transmission for our optimized Ag NW and reported electrodes (ITO,[26,27] Cu NW,[28] Ag NW,[29–31] CNT,[32–35] and Graphene[33,35–37]).

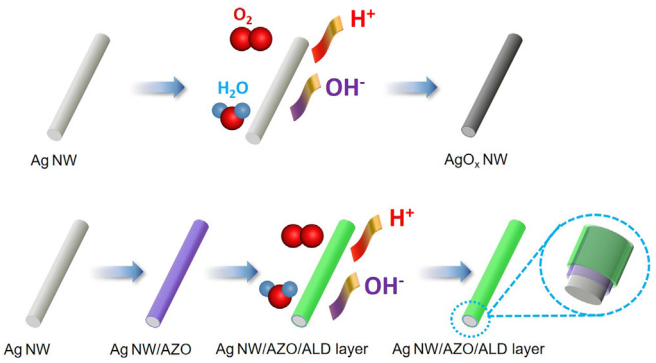

FIG. 4. Schematic diagrams of the protection mechanism for different Ag NWs.

Ag NW network, while junctions of welded Ag NWs provide enough pathways for electron transmission even after single wire breakage;[24] and (iii) compared to bare Ag NWs, the W-Ag NW/AZO/SbO_x has stronger adherence to the substrate.

The ambient stability of Ag NWs was investigated further. For 1000 h, the pristine and treated Ag NW films were exposed to the air with a constant relative humidity of 85% at 65 °C. Because of the large surface-to-volume ratio, the Ag NWs were easily oxidized when they were exposed to humid air, deteriorating the film's electrical properties, as seen in Fig. 3(f).[25] The lower cross-sectional area of Ag NWs induced by surface oxidation can explain the 30-fold increase in the sample sheet resistance.[15] However, since the Ag NWs were well protected from surface oxidation by AlO_x and SbO_x protection layers, the film sheet resistance increased marginally. Figure 3(g) illustrates the long-term stability of the Ag NW layer under ambient conditions at room temperature (RH 40%). After 6 days, the resistance of the original Ag NW layer began to deteriorate, but the conductivity of W-Ag NW/AZO/AlO_x and W-Ag NW/AZO/SbO_x remained nearly constant after 60 days.

In summary, as shown in Fig. 3(h), W-Ag NW/AZO/Al_2O_3 and W-Ag NW/AZO/SbO_x perform better than many TCE materials in terms of sheet resistance and transmittance at 550 nm. As demonstrated in Fig. 4, Ag NWs exposed to air, humidity, acidic, and alkaline solutions can be still easily degraded, deteriorating their electrical conductivity.[38] The nanogaps between the as-prepared Ag NWs impede electron transport between wires. Ethanol's capillary force might be used to weld nanowires and effectively reduce resistance. Furthermore, coating an AZO layer on Ag NWs significantly reduces the roughness of the nano-weld Ag NW layer. An ALD SbO_x encapsulation layer processed using a water-free recipe can protect the Ag NWs from oxidation and corrosion. Because SbO_x compounds have higher chemical resistance to alkaline solutions than AlO_x compounds, W-Ag NW/AZO/SbO_x films exhibit remarkable electrical stability in the solutions with pH ranging from 3 to 13.

W-Ag NW/AZO/SbO_x was employed as the gate electrode in a flexible TFT with a Ti-doped ZnO layer as the channel on the PI substrate to explore the performance of the developed layer [see Fig. 5(a)].

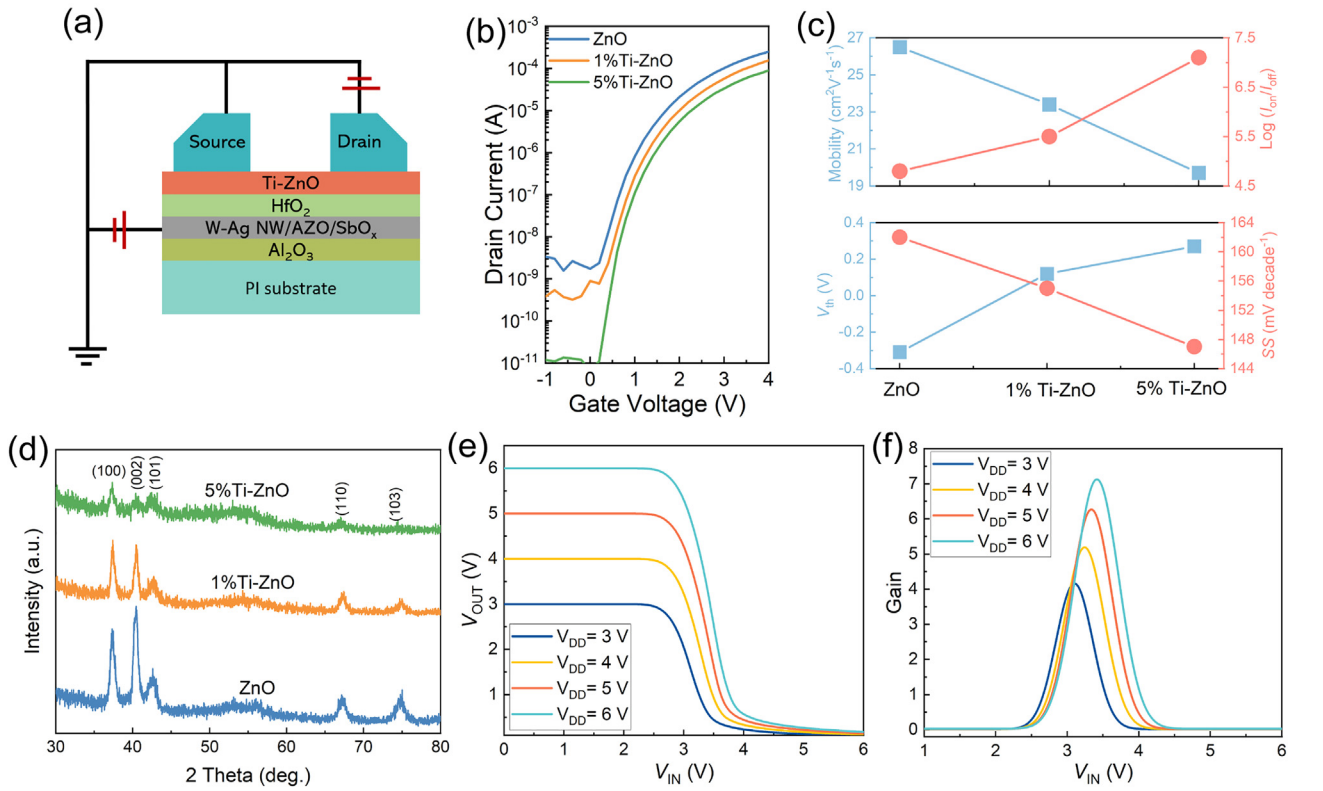

FIG. 5. (a) Schematic structure of flexible TFTs. (b) Transfer curves and (c) corresponding electrical parameters of the TFTs. (d) XRD patterns of Ti-ZnO thin films. (e) Voltage transfer characteristic curves and (f) signal gains of the inverter as a function of V_{DD}.

TABLE I. Performance parameters for TFTs with different Ti doping. (μ, V_{th}, I_{on}/I_{off}, and SS are the field-effect mobility, threshold voltage, the ratio of on and off current, and subthreshold swing, respectively).

Device	V_{th} (V)	μ ($cm^2\,V\,s^{-1}$)	I_{on}/I_{off}	SS ($mV\ decade^{-1}$)
ZnO	−0.31	26.5	10^5	162
1% Ti-ZnO	0.12	23.4	5×10^5	155
5% Ti-ZnO	0.27	19.7	10^7	147

The low roughness of the gate electrode provides an ideal surface for the deposition of a thin dielectric layer, which is required for TFTs to have high areal capacitance and low current density.[39] Figure 5(b) depicts the transfer curves of ZnO TFTs with different Ti doping. Also, the key performance parameters, including the threshold voltage (V_{th}), the field-effect mobility (μ), on/off current ratio (I_{on}/I_{off}), and subthreshold swing (SS), are calculated and presented in Table I. As Ti doping increased, the μ decreased from 26.5 to 19.7 $cm^2\,V^{-1}\,s^{-1}$, while the I_{on}/I_{off} increased from 10^5 to 10^7. The incorporation of metal cations can inhibit crystal growth in the ZnO film [see Fig. 5(d)], passivate the oxygen vacancy, control the carrier concentration, and reduce the interface trap density.[40,41] Even after 1000 cycles of bending, the TFT with the W-Ag NW/AZO/SbO_x gate electrode retained field effect mobility and showed a negligible change in the off current (Fig. S6).

The logic circuits based on Ti-ZnO TFTs were investigated further. Figure S7 shows the inverter's circuit diagram. The resistor-loaded inverter was built using 5%Ti-ZnO TFTs and a 7 MΩ external resistor. Figure 5(e) depicts the voltage transfer characteristics (VTC) at various supplied voltages (V_{DD}) ranging from 3 to 6 V with a 1 V step. The output voltages (V_{OUT}) are switched with changing V_{DD}, indicating that the inverter is performing properly with ideal swing characteristics.[42,43] The gain values (defined as $-\partial V_{OUT}/\partial V_{IN}$) were also calculated [Fig. 5(f)], and the fitted results are shown in Fig. S8. The devices exhibited a maximum gain of 7.2 at V_{DD} of 6 V. The shift in maximum gain values at different input voltages (V_{IN}) is negligible, implying that the inverter is highly stable. Continuous signal propagation in the integrated circuits requires a gain value larger than 1.[44] The device's good performance confirms that W-Ag NW/AZO/SbO_x is a promising electrode layer for integrated circuits.

In conclusion, we developed a novel method for improving the mechanical/electrical characteristics of flexible Ag NW electrodes. To begin, at room temperature, the ethanol-mist was applied to nano-weld the cross junction of the Ag NWs and reduce contact resistance. Second, an AZO solution was applied to the surface to reduce the roughness of the Ag NW thin film. Furthermore, an ultrathin SbO_x thin layer was deposited on the film surface by low-temperature ALD using a water-free recipe to passivate the charge recombination defects and prevent film electrode degradation by water or oxygen. The treated Ag NW has a high transmittance of 87% and a low sheet resistance of roughly 15 Ω/sq. The W-Ag NW/AZO/SbO_x film retains its initial conductivity even after 1000 cycles of bending testing. Furthermore, the electrode was immersed in solutions with various pH values ranging from 3 to 13 for 5 min. When compared to untreated Ag NWs or sample coated with AlO_x thin films, W-Ag NW/AZO/SbO_x shows superior electrical stability. Flexible Ti-ZnO TFTs with W-Ag NW/AZO/SbO_x gate electrodes were fabricated on a PI substrate. The field-effect mobility of 5% Ti-ZnO TFT is with 19.7 $cm^2\,V\,s^{-1}$, the I_{on}/I_{off} ratio is 10^7, and the subthreshold swing of 147 $mV\ decade^{-1}$. Ti-ZnO TFT-based inverter devices were also investigated in the current work. Our strategy adds a new dimension to the development of innovative TCE materials for high-performance flexible electronic devices.

See the supplementary material for the experimental methods and characteristics of Ag NWs and inverter devices.

This work was supported by the Program of Collaborative Research Centers in Germany (Grant No. SFB 1415).

AUTHOR DECLARATIONS

Conflict of Interest

The authors have no conflicts to disclose.

Author Contributions

Jun Yang: Investigation (equal); Methodology (equal); Writing – review & editing (lead). **Amin Bahrami:** Data curation (equal); Writing – review & editing (equal). **Xingwei Ding:** Investigation (equal); Methodology (equal). **Sebastian Lehmann:** Data curation (supporting). **Kornelius Nielsch:** Project administration (equal); Supervision (equal).

DATA AVAILABILITY

The data that support the findings of this study are available from the corresponding authors upon reasonable request.

REFERENCES

[1]Y. Ge, X. Duan, M. Zhang, L. Mei, J. Hu, W. Hu, and X. Duan, J. Am. Chem. Soc. **140**(1), 193 (2018).
[2]C. Ma, Y. F. Liu, Y. G. Bi, X. L. Zhang, D. Yin, J. Feng, and H. B. Sun, Nanoscale **13**(29), 12423 (2021).
[3]Y. N. Ding, Y. C. Cui, X. H. Liu, G. X. Liu, and F. K. Shan, Appl. Mater. Today **20**, 100634 (2020).
[4]X. Chen, G. Xu, G. Zeng, H. Gu, H. Chen, H. Xu, H. Yao, Y. Li, J. Hou, and Y. Li, Adv. Mater. **32**(14), e1908478 (2020).
[5]J. L. Wu, J. Yang, X. Y. Yang, and X. W. Ding, IEEE J. Electron Devices Soc. **8**(1), 152 (2020).
[6]V. H. Nguyen, J. Resende, D. T. Papanastasiou, N. Fontanals, C. Jimenez, D. Munoz-Rojas, and D. Bellet, Nanoscale **11**(25), 12097 (2019).
[7]S. K. Vishwanath, T. An, W. Y. Jin, J. W. Kang, and J. Kim, J. Mater. Chem. C **5**(39), 10295 (2017).
[8]P. C. Hsu, H. Wu, T. J. Carney, M. T. McDowell, Y. Yang, E. C. Garnett, M. Li, L. Hu, and Y. Cui, ACS Nano **6**(6), 5150 (2012).
[9]O. Reynaud, A. G. Nasibulin, A. S. Anisimov, I. V. Anoshkin, H. Jiang, and E. I. Kauppinen, Chem. Eng. J. **255**, 134 (2014).
[10]S. Cho, S. Kang, A. Pandya, R. Shanker, Z. Khan, Y. Lee, J. Park, S. L. Craig, and H. Ko, ACS Nano **11**(4), 4346 (2017).
[11]L. Lian, D. Dong, S. Yang, B. Wei, and G. He, ACS Appl. Mater. Interfaces **9**(13), 11811 (2017).
[12]Y. Zhuo, E. Prestat, I. A. Kinloch, and M. A. Bissett, ACS Appl. Energy Mater. **5**(1), 61 (2022).
[13]M. Vosgueritchian, D. J. Lipomi, and Z. Bao, Adv. Funct. Mater. **22**(2), 421 (2012).
[14]E. C. Garnett, W. Cai, J. J. Cha, F. Mahmood, S. T. Connor, M. Greyson Christoforo, Y. Cui, M. D. McGehee, and M. L. Brongersma, Nat. Mater. **11**(3), 241 (2012).

[15]B. Hwang, Y. An, H. Lee, E. Lee, S. Becker, Y. H. Kim, and H. Kim, Sci. Rep. **7**, 41336 (2017).
[16]M. Göbelt, R. Keding, S. W. Schmitt, B. Hoffmann, S. Jäckle, M. Latzel, V. V. Radmilović, V. R. Radmilović, E. Spiecker, and S. Christiansen, Nano Energy **16**, 196 (2015).
[17]J. Yang, A. Bahrami, X. Ding, P. Zhao, S. He, S. Lehmann, M. Laitinen, J. Julin, M. Kivekäs, and T. Sajavaara, Adv. Electron. Mater. **8**, 2101334 (2022).
[18]L. Liu, P. Gong, K. Liu, A. Nie, Z. Liu, S. Yang, Y. Xu, T. Liu, Y. Zhao, and L. Huang, Adv. Mater. **34**(7), 2106041 (2022).
[19]J. Yang, A. Bahrami, X. W. Ding, S. Lehmann, N. Kruse, S. Y. He, B. W. Wang, M. Hantusch, and K. Nielsch, Adv. Mater. Interfaces **9**(15), 2101953 (2022).
[20]Y. R. Li, B. Wang, H. Y. Hu, J. H. Zhang, B. Wei, and L. Q. Yang, IEEE Access **7**, 177944 (2019).
[21]Y. Liu, J. Zhang, H. Gao, Y. Wang, Q. Liu, S. Huang, C. F. Guo, and Z. Ren, Nano Lett. **17**(2), 1090 (2017).
[22]Y. I. Rabinovich, M. S. Esayanur, and B. M. Moudgil, Langmuir **21**(24), 10992 (2005).
[23]K. Zhang, J. Li, Y. Fang, B. Luo, Y. Zhang, Y. Li, J. Zhou, and B. Hu, Nanoscale **10**(27), 12981 (2018).
[24]S. S. Yoon and D. Y. Khang, Nano Lett. **16**(6), 3550 (2016).
[25]S. D. Standridge, G. C. Schatz, and J. T. Hupp, Langmuir **25**(5), 2596 (2009).
[26]S. Jung, S. Lee, M. Song, D. G. Kim, D. S. You, J. K. Kim, C. S. Kim, T. M. Kim, K. H. Kim, J. J. Kim, and J. W. Kang, Adv. Energy Mater. **4**(1), 1300474 (2014).
[27]D. H. Wang, A. K. K. Kyaw, V. Gupta, G. C. Bazan, and A. J. Heeger, Adv. Energy Mater. **3**(9), 1161 (2013).
[28]Y. Yu, Y. Zhang, K. Li, C. Yan, and Z. Zheng, Small **11**(28), 3444 (2015).
[29]M. S. Miller, J. C. O'Kane, A. Niec, R. S. Carmichael, and T. B. Carmichael, ACS Appl. Mater. Interfaces **5**(20), 10165 (2013).
[30]J. H. Yoo, Y. Kim, M. K. Han, S. Choi, K. Y. Song, K. C. Chung, J. M. Kim, and J. Kwak, ACS Appl. Mater. Interfaces **7**(29), 15928 (2015).
[31]J. Lee, P. Lee, H. B. Lee, S. Hong, I. Lee, J. Yeo, S. S. Lee, T. S. Kim, D. Lee, and S. H. Ko, Adv. Funct. Mater. **23**(34), 4171 (2013).
[32]J. Y. Lee, S. T. Connor, Y. Cui, and P. Peumans, Nano Lett. **8**(2), 689 (2008).
[33]Z. Wu, Z. Chen, X. Du, J. M. Logan, J. Sippel, M. Nikolou, K. Kamaras, J. R. Reynolds, D. B. Tanner, A. F. Hebard, and A. G. Rinzler, Science **305**(5688), 1273 (2004).
[34]S. De, P. E. Lyons, S. Sorel, E. M. Doherty, P. J. King, W. J. Blau, P. N. Nirmalraj, J. J. Boland, V. Scardaci, J. Joimel, and J. N. Coleman, ACS Nano **3**(3), 714 (2009).
[35]V. C. Tung, L. M. Chen, M. J. Allen, J. K. Wassei, K. Nelson, R. B. Kaner, and Y. Yang, Nano Lett. **9**(5), 1949 (2009).
[36]K. S. Kim, Y. Zhao, H. Jang, S. Y. Lee, J. M. Kim, K. S. Kim, J. H. Ahn, P. Kim, J. Y. Choi, and B. H. Hong, Nature **457**(7230), 706 (2009).
[37]S. Bae, H. Kim, Y. Lee, X. Xu, J. S. Park, Y. Zheng, J. Balakrishnan, T. Lei, H. R. Kim, Y. I. Song, Y. J. Kim, K. S. Kim, B. Ozyilmaz, J. H. Ahn, B. H. Hong, and S. Iijima, Nat. Nanotechnol. **5**(8), 574 (2010).
[38]Y. Cui, Y. Meng, Z. Wang, C. Wang, G. Liu, R. Martins, E. Fortunato, and F. Shan, Nanoscale **10**(41), 19427 (2018).
[39]J. Yang, Y. P. Zhang, Q. Q. Wu, C. Dussarrat, J. Qi, W. Q. Zhu, X. W. Ding, and J. H. Zhang, IEEE Trans. Electron Devices **66**(8), 3382 (2019).
[40]A. Abliz, D. Wan, L. Yang, M. Mamat, H. Chen, L. Xu, C. Wang, and H. Duan, Mater. Sci. Semicond. Process. **95**, 54 (2019).
[41]J. Yang, Y. P. Zhang, C. P. Qin, X. W. Ding, and J. H. Zhang, IEEE Trans. Electron Devices **66**(4), 1760 (2019).
[42]C. Fan, A. Liu, Y. Meng, Z. Guo, G. Liu, and F. Shan, IEEE Trans. Electron Devices **64**(10), 4137 (2017).
[43]J. Li, D.-Y. Zhong, C.-X. Huang, X.-F. Li, and J.-H. Zhang, IEEE Trans. Electron Devices **65**(7), 2838 (2018).
[44]Y. Liu, X. Wan, L. Q. Zhu, Y. Shi, and Q. Wan, IEEE Electron Device Lett. **35**(12), 1257 (2014).